

# Diffusive mixing between shearing granular layers: constraints on bed deformation from till contacts

THOMAS S. HOOYER,\* NEAL R. IVERSON

*Department of Geological and Atmospheric Sciences, Iowa State University, Ames, Iowa 50011, U.S.A.*

**ABSTRACT.** Shearing of subglacial till has been invoked widely as a mechanism of glacier motion and sediment transport, but standard indicators for determining shear strain from the geologic record are not adequate for estimating the very high strains required of the bed-deformation model. Here we describe a laboratory study of mixing between shearing granular layers that allows an upper limit to be placed on bed shear strain in the vicinity of till contacts. Owing to random vertical motions of particles induced by shearing, mixing can be modeled as a linearly diffusive process, and so can be characterized with a single mixing coefficient,  $D$ . Ring-shear experiments with equigranular beads and lithologically distinct tills provide the value of  $D$ , although in experiments with till  $D$  decreases systematically with strain to a minimum value of  $0.0045 \text{ mm}^2$ . Kinetic gas theory provides an estimate of the dimensionless mixing coefficient which is within an order of magnitude of laboratory values. Knowing the minimum value of  $D$ , the distribution of index lithologies measured across till contacts in the geologic record can be used to estimate the maximum shear strain that has occurred across till contacts. Application of this technique to the contact between the Des Moines and Superior Lobe tills in east-central Minnesota, U.S.A., indicates that shear strain did not exceed 15 000 at the depth of the contact.

## INTRODUCTION

Pervasive deformation of water-saturated subglacial till has been suggested as the primary mechanism of glacier motion and sediment transport (Alley, 1991; Clark, 1994; Jenson and others, 1995, 1996; Boulton, 1996; Clark and others, 1996; Hooke and Elverhøi, 1996; Dowdeswell and Siegert, 1999). This process may have occurred beneath the southern margin of the Laurentide ice sheet, where laterally extensive sheets of generally fine-grained till overlie bedrock (e.g. Clark and Walder, 1994; Clark, 1997). Many field studies of Pleistocene tills have attempted to establish sedimentological criteria for deformation (e.g. Hicock and Dreimanis, 1992; Menzies and Maltman, 1992; Hart, 1994, 1997; Hart and Roberts, 1994). Convincing observations from some of these studies include microstructural rotational features and shear bands (Van der Meer, 1993, 1997; Menzies and others, 1997), folds and boudinage (Hart and Boulton, 1991; Hart and Roberts, 1994), grain fracturing (Hiemstra and van der Meer, 1997) and deformed pods of sorted sediment incorporated within basal tills (Hart, 1995; Piotrowski and Kraus, 1997). These features, however, either do not provide a quantitative means of estimating shear strain or should be obliterated at the high shear strains required of the bed-deformation model.

It is important to keep in mind the very high shear strains that should result from glacier motion accommodated primarily by bed deformation. For example, if we consider

an ice sheet that moves at its base at a speed of  $400 \text{ m a}^{-1}$  and shears its bed to 5 m depth for 1000 years, the resultant shear strain, averaged over the deforming-till thickness, would be 80 000. Thus, efforts to distinguish moderate strains from very high strains in the bed are important.

Efforts have recently been made to determine if the alignment of gravel-sized clasts in till can be used to estimate strain magnitude (Hooyer and Iverson, 2000). The results of laboratory experiments indicate that strong fabrics develop in the direction of shearing at relatively small shear strains (1–2) and remain strong at progressively higher strains. Thus, although useful in determining whether a till has been deformed to a strain larger than  $\sim 1.0$ , this method cannot be used to identify tills sheared to the very high strains required to account for significant glacier motion.

One sedimentological characteristic that has been used as evidence both for and against deformation is the visually sharp contact that is often observed between basal till units and underlying sediment. Kemmis (1981) and Clayton and others (1989) argued that pervasive deformation would cause mixing, thereby resulting in a gradational contact. In contrast, Alley (1991) suggested that sharp contacts might be the result of deformation. He suggested that, owing to the expected downward increase in effective pressure (the difference between the total normal stress and pore-water pressure), till at some critical depth would shear too slowly to maintain its high porosity, and thus compact, strengthen, and stop shearing. This effect might result in a sharp contact between the upper deforming layer and underlying rigid layer and could, if provenance changed, superpose tills of different compositions.

This study focuses on mixing between lithologically dis-

\* Present address: Wisconsin Geological and Natural History Survey, 3817 Mineral Point Road, Madison, Wisconsin 53705, U.S.A.

tinct tills and other more ideal granular materials undergoing slow, steady, bed-parallel shearing. Our approach is to use a rotary device that shears granular materials to various strains under conditions similar to those beneath modern glaciers. The results indicate that mixing between granular layers, including tills, is proportional to the cumulative strain and can be modeled as a diffusive process. Consequently, the extent of mixing across a stratigraphic contact provides a useful constraint on shear strain in the vicinity of the contact. The method is illustrated by applying it to two tills in stratigraphic contact in east-central Minnesota, U.S.A.

**THEORY**

During shearing of a granular material, grains climb over adjacent grains and fall into void spaces, and thus most grains at any instant have a component of their motion normal to the shearing direction. This is true regardless of whether the material expands, contracts or maintains a steady volume during shearing. If these grain motions are essentially random, then diffusive transport of grains normal to the shearing direction is expected.

Consider two granular layers of combined thickness  $h$  in a section oriented normal to the shearing direction, where  $z$  is the distance from the top of the shear zone (Fig. 1a). Define an index lithology that is significantly more abundant in one layer than the other. The dimensionless concentration of this lithology  $C$  is defined as the number of index grains divided by the total number of grains. If during shearing the vertical flux of index grains associated with mixing scales linearly with  $\partial C/\partial z$ , then

$$\frac{\partial C}{\partial \gamma} = D \frac{\partial^2 C}{\partial z^2}, \tag{1}$$

where  $D$  is a mixing coefficient and  $\gamma$  is shear strain. This is Fick’s second law written in terms of  $\gamma$ , rather than time. Consequently,  $D$  has the dimensions  $m^2$ . If  $C_1$  and  $C_2$  are the initial dimensionless concentrations of the index lithology in the upper and lower layers, respectively,  $z_0$  is the position of the contact between the two layers and there is no flux out of the shear zone, then appropriate initial and boundary conditions are as follows:

$$\begin{aligned} C &= C_1 \quad \text{for} \quad 0 < z < z_0, \quad \gamma = 0; \\ C &= C_2 \quad \text{for} \quad z_0 < z < h, \quad \gamma = 0; \end{aligned} \tag{2}$$

$$\begin{aligned} \frac{\partial C}{\partial z} &= 0 \quad \text{for} \quad z = 0, \quad \gamma > 0; \\ \frac{\partial C}{\partial z} &= 0 \quad \text{for} \quad z = h, \quad \gamma > 0. \end{aligned} \tag{3}$$

If  $C_1 > C_2$ , there is downward diffusion of the index lithology, and the solution to Equation (1) is

$$\begin{aligned} C(z, \gamma) &= C_1 C_2 + \frac{C_1 z_0}{h} + \frac{2C_1}{\pi} \sum_{m=1}^{\infty} \frac{\exp\left[-Dm^2\pi^2\left(\frac{\gamma}{h^2}\right)\right]}{m} \\ &\cdot \cos\left(\frac{m\pi z}{h}\right) \sin\left(\frac{m\pi z_0}{h}\right) \end{aligned} \tag{4}$$

(Shackelford, 1991). Figure 1b illustrates solutions for several values of  $\gamma$ . The approach taken here is to determine  $D$  by measuring mixing between two till layers in ring-shear tests in which all other variables in Equation (4) are known. Variations in the concentration of index lithologies across till contacts in the field can then, in principle, be used to constrain the value of  $\gamma$ .

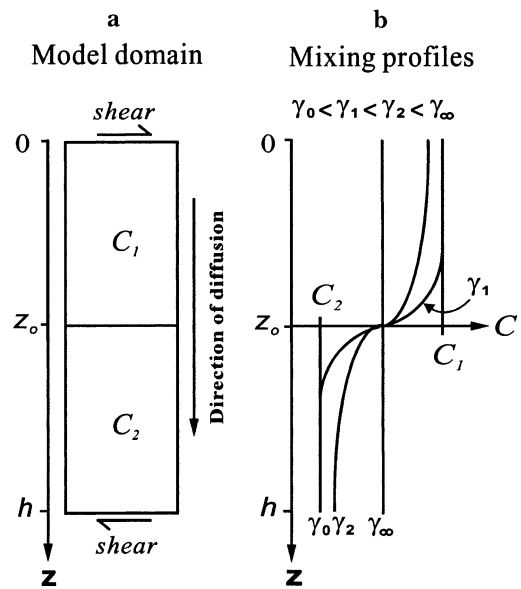


Fig. 1. Mixing model schematic of (a) the model domain, and (b) the concentration of an index lithology across the shear zone as a function of shear strain.

**APPARATUS**

Our ring-shear device (Fig. 2a) shears an annular sediment specimen at a constant rate between horizontal, parallel platens (Iverson and others, 1997, 1998). A steady stress is applied normal to the shearing direction. The rotary design of the device allows experiments to be carried out to high shear strains, and its transparent outer walls allow mixing at the outer edge of the specimen to be observed continuously during shearing. In addition, the device is sufficiently large to accommodate till specimens with gravel-size clasts.

The sediment specimen occupies an annular chamber that has an outside diameter of 0.6 m, a width of 0.115 m and a height of 0.085 m (Fig. 2b). Both the upper and lower platens contain teeth (not shown), 6 mm high, that grip the specimen during shearing. These platens are permeable and connected to an internal water reservoir that is open to the atmosphere. The lower platen is connected to a thick base plate, and the sediment is sheared by rotating this plate with a variable-speed motor and gearboxes. The upper platen is attached to a thick aluminum plate, called the normal-load plate, that is fixed rotationally by two diametrically opposed load cells secured to the frame of the device. The normal-load plate can move freely up or down if the specimen thickness changes during shearing. A downward force is applied to this plate and transferred to the specimen with dead weights suspended on a hanger attached to the end of a lever arm. The specimen is confined on its sides by stationary upper walls and by lower walls connected to the base plate. Thus, the lower walls slide beneath the upper walls during shearing (Fig. 2b).

**METHODOLOGY**

Mixing experiments were performed with two sets of materials: spherical glass beads of uniform size (0.8 mm in diameter) but different color, and two late Wisconsin-age tills with distinct lithologies. Initial experiments with beads provided simple tests of whether mixing can be modeled successfully as a diffusive process. Subsequent experiments were with tills from east-central Minnesota: the red Superior

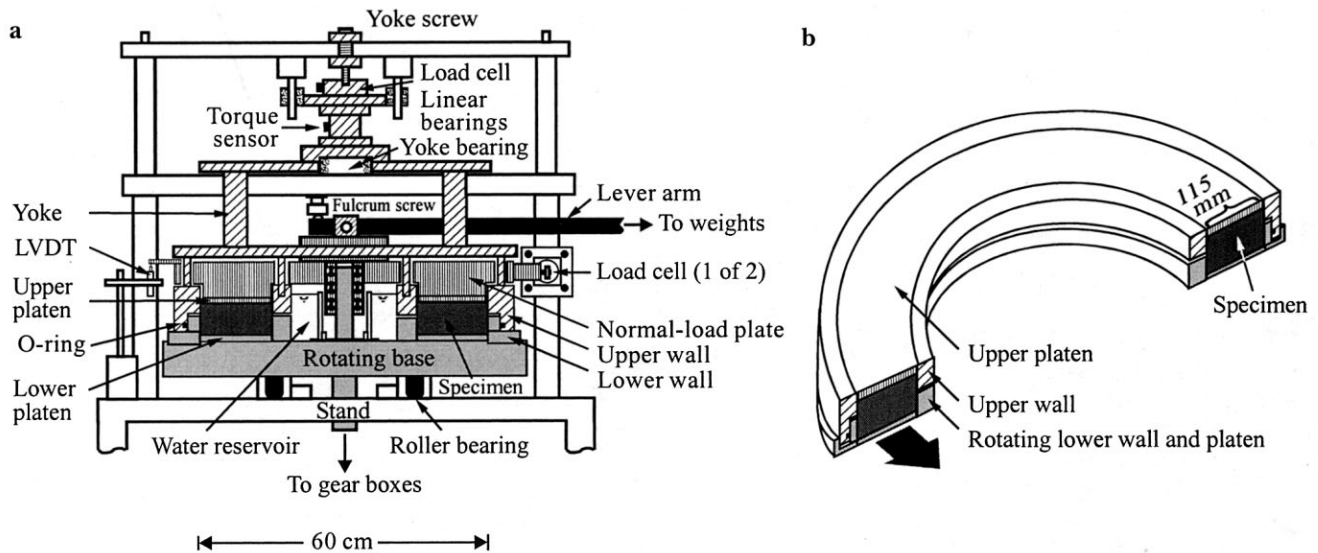


Fig. 2. (a) Cross-section of the ring-shear device, and (b) schematic of the specimen chamber. Lightly shaded components rotate.

Lobe till and the gray Des Moines Lobe basal till. The latter directly overlies the former and was deposited by the Grantsburg Sublobe, a northeastern arm of the Des Moines Lobe of the Laurentide ice sheet. The tills have similar grain-size distributions (Fig. 3), although the Des Moines Lobe till (16% clay, 36% silt, 40% sand and 8% gravel) is somewhat finer-grained than the Superior Lobe till (12% clay, 31% silt, 51% sand and 6% gravel). The Des Moines Lobe till was deposited by ice that advanced from the northwest, and is enriched in Cretaceous shale and Paleozoic carbonates. The Superior Lobe advanced from the northeast out of the Lake Superior basin and deposited a till that is devoid of shale and relatively enriched in Precambrian igneous rocks and Cambrian sandstone (Chernicoff, 1983).

In each of four experiments with beads, a 35–40 mm thick layer of red beads is placed inside the sample chamber. The top of this layer is smoothed, and a second layer of white beads, similar in thickness, is added, forming a sharp, relatively smooth contact between the two layers (Fig. 4a). Vertical columns of displacement markers, spherical wooden beads 2–4 mm in diameter, are then placed across the width of the specimen to assess the distribution of shear strain. A normal stress of 85 kPa is then applied, and the specimen is sheared at a steady rate of  $365 \text{ m a}^{-1}$  to a predetermined displacement. These values are similar to those of some glaciers, if normal stress and shearing rate are equated with the effective normal stress on the bed and the rate of basal

motion, respectively. The experiments were performed dry, although the behavior of granular materials, including beads, is not expected to be different under water-saturated, fully drained conditions (Lambe and Whitman, 1969, p. 304). After shearing is complete, the device is disassembled, and the locations of the displacement markers are measured. At two locations within the chamber, bead samples are collected at approximately 1 mm intervals through the thickness of the specimen to document mixing (Fig. 4b). They are collected using a thin plate, 30 mm  $\times$  50 mm, with adhesive tape on one side. The plate is gently lowered onto the center line of the specimen. Upon removal of the plate, approximately 2000–4000 beads are stuck to the adhesive tape. No beads within 40 mm of the walls are sampled. Each bead sample is split multiple times to obtain a representative sample of 200–500 beads that are subsequently identified by color under a binocular microscope. The relative concentrations of white beads are plotted as a function of depth. Resultant profiles are referred to, hereafter, as mixing profiles.

The procedure in the till experiments is similar to that of the bead experiments except that the till layers are fully saturated with water upon application of the normal load, and consolidation is allowed to occur prior to shearing. In addition, all clasts larger than 8 mm are removed from both tills in accordance with geotechnical testing procedures outlined by Head (1989, p. 83). These clasts represent approximately 2.0% and 1.2% of the Des Moines and Superior Lobe tills by volume, respectively. The Superior Lobe till is then placed in the sample chamber beneath the Des Moines Lobe till. As in the bead experiments, the contact between the two tills is made as smooth and sharp as possible, and vertical columns of displacement markers are inserted in the till to assess the distribution of shear strain at the ends of experiments. After an experiment is complete, two blocks of intact till are removed from the chamber, and a guided metal scraper is used to collect samples at 1 mm intervals. Each sample is then wet-sieved to separate the 0.4–1.0 mm grain-size fraction. These grains are large enough to identify easily, but small enough to provide a large sample (150–500) for identification.

To quantify mixing in the till experiments, a suitable index lithology must be selected. Shale is a good choice due to its abundance in the Des Moines Lobe till and its absence in the Superior Lobe till. The mean shale content of the Des Moines

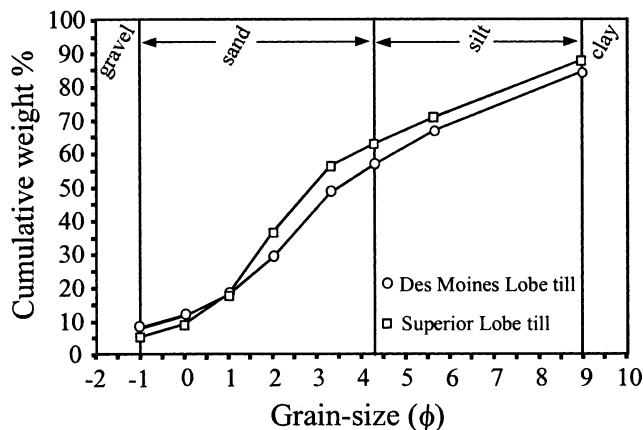


Fig. 3. Particle-size distributions of the Des Moines Lobe and Superior Lobe tills.

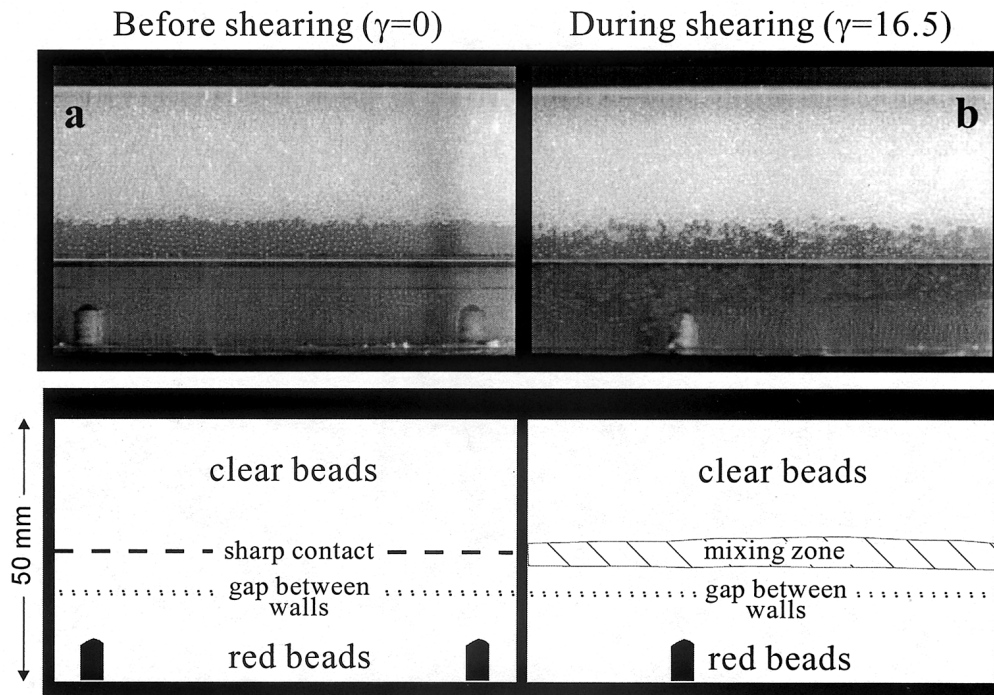


Fig. 4. Photographs taken through the transparent outer wall of the ring-shear device during a bead experiment. (a) Contact before shearing, and (b) zone of mixing during shearing.

Lobe till in the 0.4–1.0 mm grain-size fraction is 9–12%. A binocular microscope is used to identify and count shale grains and the total number of grains in each sample.

Equation (4) is fit to mixing profiles from both the bead and till experiments, considering only its first 25 terms, to determine the mixing coefficient,  $D$ . Other variables in Equation (4) are well constrained. The thickness of the shear zone and the total shear strain are determined from the final locations of the displacement markers. Note that as boundary conditions, Equations (3) apply because there will not be transport of sediment outside the upper and lower boundaries of the shear zone. The initial concentrations of shale in the two tills ( $C_1$  and  $C_2$ ) are determined from grain counts of till samples collected prior to shearing and from undeformed portions of the specimen after shearing. Although the height of the initial contact,  $z_0$ , is measured prior to shearing, the measurement does not account for small undulations in the initial contact and changes in specimen thickness that occur during consolidation and shearing. Therefore,  $z_0$  is determined from the resulting mixing profiles as the height at which the dimensionless white bead or shale concentration equals 0.5.  $D$  is determined by minimizing the sum of the residuals between the modeled and observed concentration data. The goodness of fit of the model prediction to the data is evaluated using the coefficient of determination,  $r^2$ , calculated in the usual way (Steel and others, 1997). One to three  $D$  values, each corresponding to a different sampling location, are determined for each experiment. A mean value of  $D$  and a 95% confidence interval are determined from these values if there was more than one sampling location, as was the case in most experiments.

## RESULTS

### Strain distribution

To determine  $D$ , the distribution of strain needs to be documented. The final locations of displacement markers near

the center of the specimen in representative bead and till experiments are shown in Figure 5a. In both materials, the shear zone is always sandwiched between zones of negligible deformation where there is no detectable relative displacement between markers. These zones of negligible deformation form due to friction between the specimen and the walls (Iverson and others, 1997). The shear zones vary slightly in vertical position, and their thickness is 22–32.5 mm in the beads and 28–41 mm in the till. Shear strains are calculated using the shear-zone thickness and the total displacement of the lower platen at the specimen center line. Strain across the shear zones is linearly distributed approximately (Fig. 5a). This cannot be documented in tests carried out to higher strains, because in such tests the lower platen completes more than one revolution, so the number of complete revolutions by any one marker in the shear zone is equivocal. Nevertheless, in such tests the shear-zone thickness can be determined from markers excavated above and below the shear zone (Fig. 5b; see also Hooyer, 1999).

The shear-zone thickness decreases slightly across the width of both the bead and till specimens from the sample center line to the outer walls (Fig. 6). Thus, all samples used to establish the mixing profiles were collected over a 30–40 mm wide area in the middle of the specimen where the shear-zone thickness was essentially uniform.

### Mixing

The mixing profiles for the bead and till experiments are presented in Figures 7 and 8, respectively. The parameter values for the experiments, including  $h$ ,  $\gamma$  and the shear strain rate,  $\dot{\gamma}$ , are summarized in Table 1. The different symbols in Figures 7 and 8 represent different sampling locations. The curves are fits of the diffusion model to the data in which the only fitted variable is  $D$ . The  $r^2$  values indicate a generally good correlation between the modeled and observed concentrations. To compare  $D$  values for the bead and till experiments, a dimensionless mixing coefficient,  $D^*$ , is determined by dividing  $D$

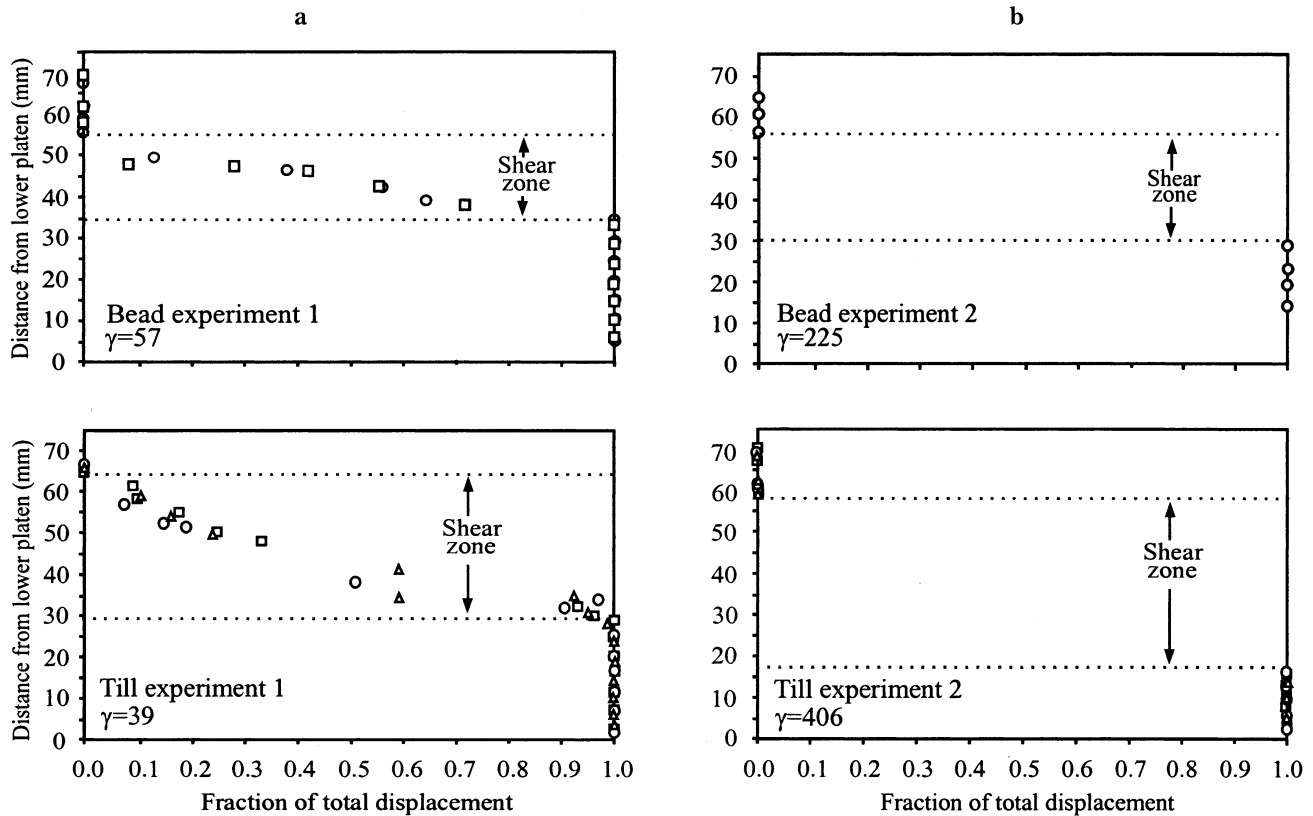


Fig. 5. Profiles of longitudinal displacement in experiments with beads and till carried out to (a) strains sufficiently small that displacements of all markers could be determined unequivocally and (b) larger strains in which displacements of markers in the shear zone could not be determined with certainty.

by the square of the diameter of particles that were counted. For the till, this size was 0.4–1.0 mm, so an average value of 0.7 mm is used. Values of  $D$ ,  $D^*$ ,  $z_0$  and  $r^2$  for each experiment are summarized in Table 2. Despite the different grain-size distributions of the beads and till, average  $D^*$  values for the two materials are quite similar: 0.11 and 0.15 for the beads and till, respectively.

Mean values of  $D^*$  for each test, determined by averaging values of  $D^*$  determined at each sampling position, are plotted with 95% confidence intervals as a function of shear strain in Figure 9. Mean  $D^*$  values from the four bead experiments do not vary systematically with strain, and range from 0.039 to 0.219. Mean  $D^*$  values from the till

experiments, however, decrease monotonically with strain from 0.378 to 0.014.

## DISCUSSION

### Laboratory results

These experiments demonstrate that mixing occurs between adjacent layers of granular material as they are sheared slowly, and that this mixing can be modeled as a one-dimensional diffusive process. As noted earlier, this implies that the vertical component of particle motion is essentially random and that the associated flux of particles is

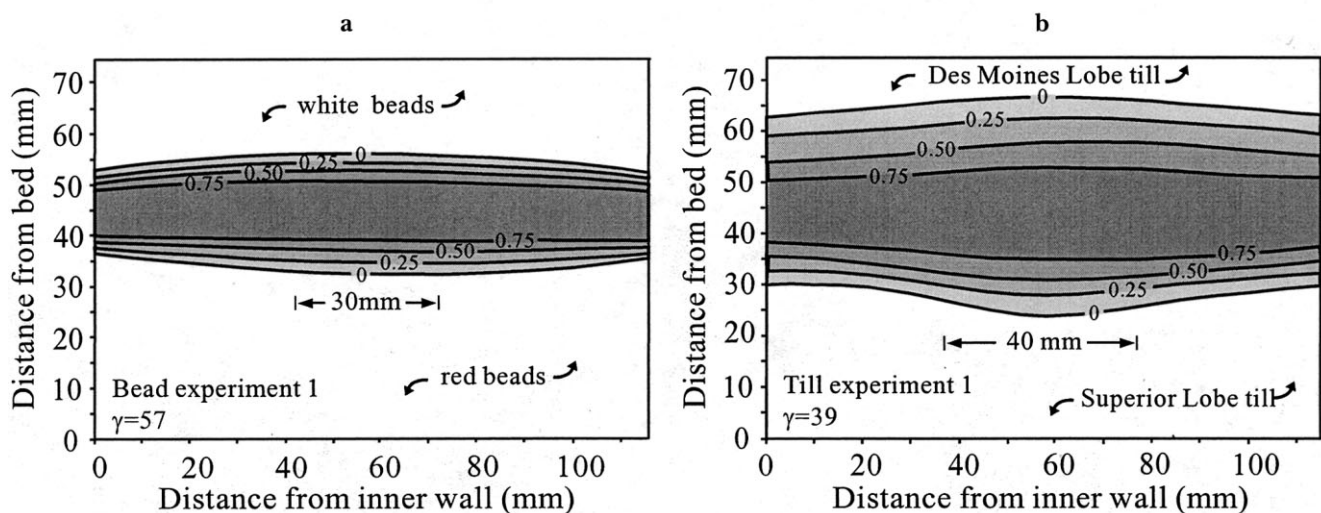


Fig. 6. Distribution of shear strain in transverse cross-section in (a) a bead experiment and (b) a till experiment. Shear strain has been normalized to the total cumulative strain at each position across the specimen width. Grains were collected from the middle of the specimen over widths of 30 and 40 mm in the bead and till experiments, respectively.

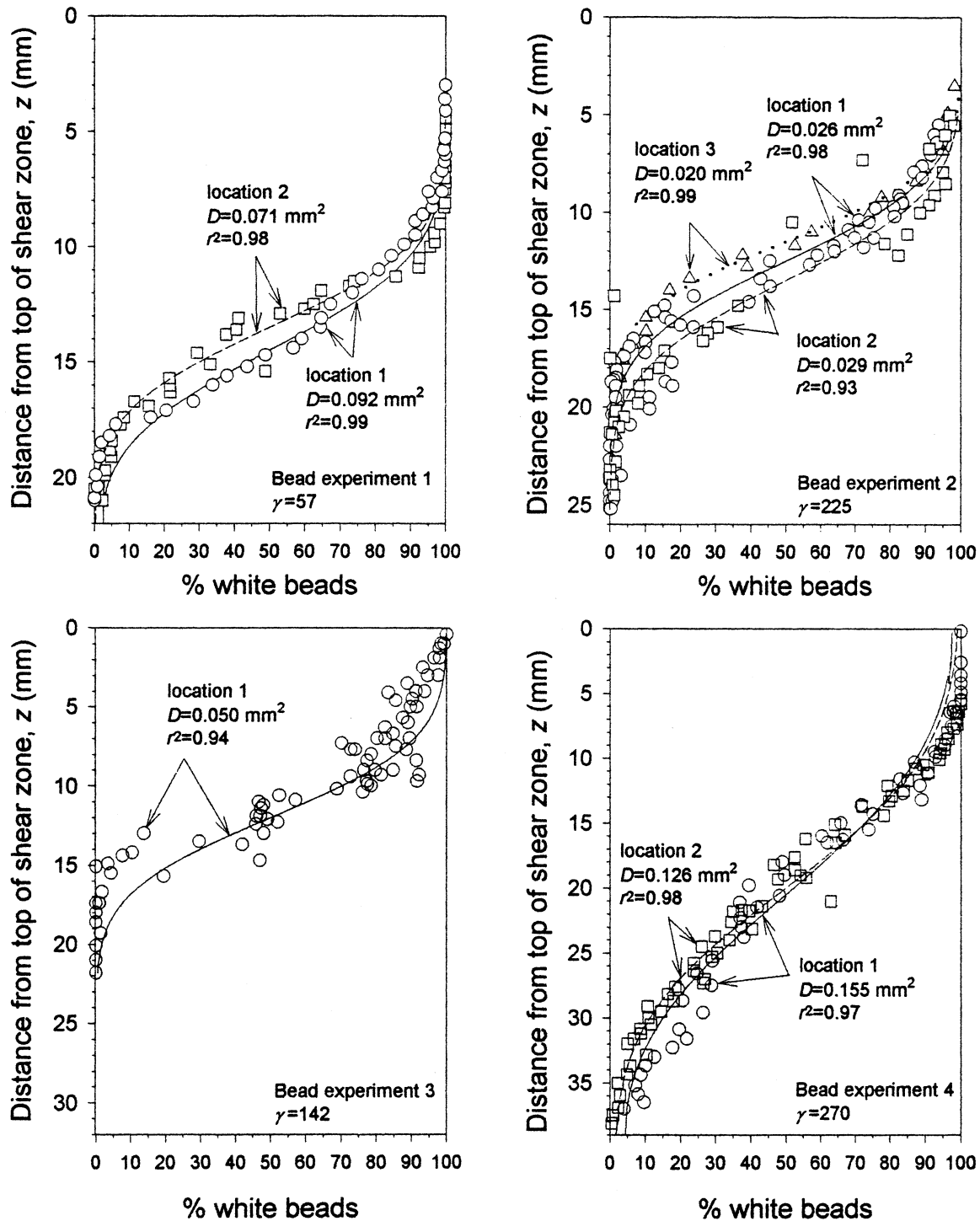


Fig. 7. Mixing profiles for bead experiments 1–4, each carried out to a different shear strain. The different vertical scales result from the different shear-zone thicknesses.  $D$  is determined by optimizing the fit of Equation (4) to the data, as indicated. In experiment 3, three sampling locations were combined into one profile due to difficulties with bead identification caused by the removal of the beads' colored surface coating during shearing.

proportional to the concentration gradient of a particular index lithology.

$D^*$  values from the bead experiments vary through less than an order of magnitude and do not vary systematically with strain, but those from the till experiments vary through a factor of 27 and decrease with strain. This implies that either diffusion of particles in the till is fundamentally non-linear, or some condition of the theory was imperfectly satisfied during the till experiments.

There are two possible explanations for the decrease in  $D^*$  with strain in the till experiments that do not involve non-linear diffusion. First, the sharp contact between the two tills may become irregular if consolidation prior to

shearing is non-uniform. An irregular initial contact would result in artificially large  $D^*$  values in experiments terminated at low strains. In experiments carried out to higher strains, the apparent mixing resulting from an irregular contact would be a smaller fraction of the total mixing, so  $D^*$  values calculated from such experiments would be smaller and would more accurately reflect the diffusive particle flux. A second possibility is that at large strains deformation becomes focused high in the shear zone, as was observed in experiments by Mandl and others (1977) on various granular materials with a similar ring-shear device. This would lead to artificially low  $D^*$  values at high strains because till at greater depths in the shear zone where mixing occurs would be

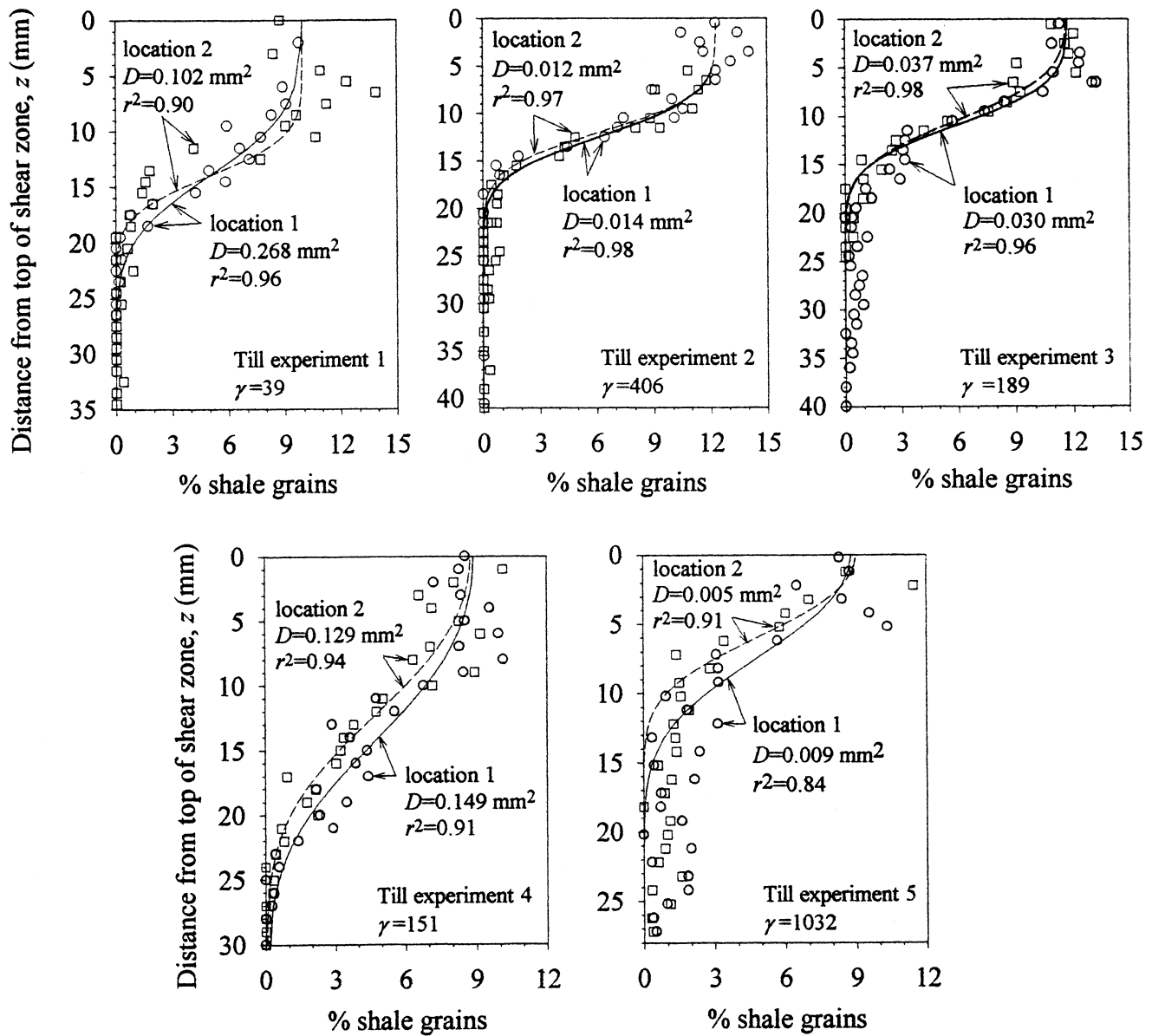


Fig. 8. Mixing profiles for till experiments 1–5, each carried out to a different shear strain. The different vertical scales result from the different shear-zone thicknesses. The mixing coefficient,  $D$ , is determined by optimizing the fit of Equation (4) to the data, as indicated.

subjected to a smaller cumulative strain than that used in the determination of  $D^*$ . This possibility cannot be ruled out, because the uniformity of strain across the shear zones can be verified only at low strains (Fig. 5).

Despite the vastly different grain-size distributions of the beads and till, average  $D^*$  values for the two materials differ by only 30%. Apparently, the ensemble average of vertical particle motions induced by shearing was not greatly differ-

Table 1. Experimental parameters

Experiment No.	Shear zone boundary* mm	Shear zone thickness, $h$ mm	Initial shale conc. %	Total displacement at sample center mm	Shear strain, $\gamma$	Elapsed time of experiment s	Shearing rate $\text{mm s}^{-1}$	Average shear strain rate, $\dot{\gamma}$ $\text{s}^{-1}$
Bead 1	35–57	22	N/A	1245	57	88 320	0.014	$6.41 \times 10^{-4}$
Bead 2	32–56	26	N/A	5846	225	456 420	0.013	$4.93 \times 10^{-4}$
Bead 3	24–56	32	N/A	4550	142	359 820	0.013	$3.95 \times 10^{-4}$
Bead 4	20–59	39	N/A	10 518	270	716 400	0.015	$3.76 \times 10^{-4}$
Till 1	29–64	35	9.9	1355	39	108 120	0.013	$3.58 \times 10^{-4}$
Till 2	17–58	41	12.3	16 636	406	623 040	0.027	$6.51 \times 10^{-4}$
Till 3	20–60	40	11.7	7558	189	601 620	0.013	$3.14 \times 10^{-4}$
Till 4	29–59	30	9.2	4522	151	346 560	0.013	$4.35 \times 10^{-4}$
Till 5	26–54	28	9.6	28 915	1032	2 093 940	0.013–0.016	$5.10 \times 10^{-4}$

\* Distance above bottom platen.

N/A, not applicable.

Table 2. Experimental results

Experiment No.	Sample location	Initial contact height, $z_0$	$D$	$D^*$	$r^2$
		mm	mm <sup>2</sup>		
Bead 1	1	14.5	0.092	0.144	0.99
	2	13.5	0.071	0.111	0.98
Bead 2	1	13.5	0.026	0.041	0.98
	2	12.5	0.029	0.045	0.93
	3	14.5	0.020	0.031	0.99
Bead 3	1	12.0	0.050	0.078	0.94
Bead 4	1	20.5	0.155	0.242	0.97
	2	20.0	0.126	0.197	0.98
Till 1	1	14.0	0.268	0.547	0.96
	2	14.0	0.102	0.210	0.90
Till 2	1	12.5	0.014	0.029	0.98
	2	12.0	0.012	0.024	0.97
Till 3	1	11.0	0.030	0.061	0.96
	2	10.5	0.037	0.076	0.98
Till 4	1	14.5	0.149	0.304	0.91
	2	12.5	0.129	0.264	0.94
Till 5	1	7.5	0.009	0.018	0.84
	2	6.0	0.005	0.010	0.91

ent in the two materials. In addition, the till did not undergo detectable percolation (Scott and Bridgwater, 1976; Stephens and Bridgwater, 1978; Bridgwater and others, 1985; Savage, 1987), the process by which smaller particles move down through void spaces created by a network of larger particles during shearing. Percolation was not important in our experiments because >80% of till particles were smaller than the 0.4–1.0 mm shale grains that were counted to establish the mixing profiles. These shale grains, therefore, were surrounded by predominantly smaller particles, and thus void spaces large enough to allow their percolation were probably rare. Furthermore, if percolation of shale particles did occur, till mixing profiles should have displayed systematic asymmetry. No such asymmetry was observed.

Values of  $D^*$  indicated by our experiments are similar to those determined by others (Scott and Bridgwater, 1976; Stephens and Bridgwater, 1978; Bridgwater, 1980). In the experiments of Scott and Bridgwater (1976), a simple-shear apparatus was used to study the mixing between two layers of spheres of different color undergoing shear. Stephens and Bridgwater (1978) conducted a similar experiment with an annular shear device. The equivalent mean  $D^*$  values from these studies were 0.022–0.055 and fall within the range of values determined from our bead and till experiments (Table 2).

The similarity between  $D^*$  values from these studies and those from our experiments is significant because these studies were carried out at much higher strain rates (0.161–3.8 s<sup>-1</sup>) and lower normal stresses (1.36–3.42 kPa). To quantify the difference in momentum exchange and friction between these laboratory studies and our experiments, we calculated Savage numbers (see Iverson, 1997), the ratio of inertial shear stress associated with grain collisions to the quasi-static shear stress associated with grain friction. Savage numbers from our experiments were at least eight orders of magnitude smaller than those calculated for natural and experimental debris flows (Iverson, 1997) and from laboratory experiments (Scott and Bridgwater, 1976; Stephens and Bridgwater, 1978). The apparent insensitivity of  $D^*$  values to both strain rate and effective normal stress indicates that our experimental  $D^*$

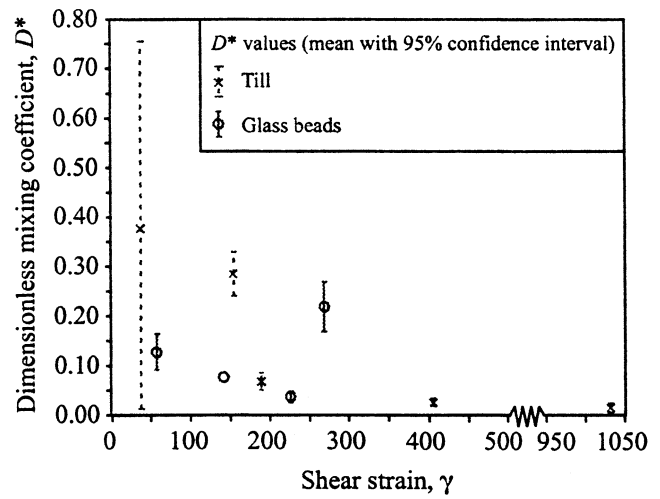


Fig. 9. Dimensionless mixing coefficient,  $D^*$ , as a function of shear strain for the bead and till experiments.

values can be applied to subglacial settings where strain rates and effective pressures may have been different from those of our experiments.

The  $D^*$  values determined from our experiments are also similar to those calculated using kinetic gas theory. Kinetic theory has been used extensively to model granular flows (Savage and Jeffery, 1981; Jenkins and Savage, 1983; Lun and others, 1984; Hsiau and Hunt, 1993; Savage, 1993) because of their similarities to the flow of gases and dense fluids at the molecular level. Particles in a shearing granular material are in an agitated state of motion and experience frequent collisions with surrounding particles. If the velocity of individual particles after a collision is  $u$ , and the average velocity of all particles is  $c$ , then a quantity called the granular temperature,  $T$ , can be defined for uniform simple shear:

$$T = \frac{C^2}{3}, \tag{5}$$

where  $C$  is the average difference between  $c$  and  $u$  (Lun and others, 1984). Knowing the diameter of the particles,  $\sigma$  and the coefficient of restitution,  $e$ , that characterizes the elasticity of the particle collisions, then the diffusivity determined from kinetic theory,  $D_k$ , is

$$D_k = \frac{\sigma\sqrt{\pi T}}{8(1+e)v_{g0}}, \tag{6}$$

where  $g_0$ , the so-called radial-distribution function, represents the velocity distribution of particles in contact with each other (Hsiau and Hunt, 1993; Savage, 1993). An empirical approximation of  $g_0$  is given by Carnahan and Starling (1969):

$$g_0 = \frac{(2-v)}{2(1-v)^3}, \tag{7}$$

where  $v$  is the bulk solid fraction of the granular material during shearing ( $1 - \text{porosity}$ ). The parameters used to calculate values of  $D_k$  are presented in Table 3. A reasonable upper bound for  $u$  in our experiments is the displacement rate of the rotating lower platen, and a reasonable value for  $c$  is one-half the displacement rate of the lower platen. Data and analysis presented by Lun and Savage (1986) suggest that  $e$  approaches 1.0 if the impact velocity between particles is small, as in our experiments. Thus,  $0.85 < e < 1.0$  is assumed. The measured bulk density is used to determine  $v$ . To facilitate comparison with our laboratory results, values of  $D_k$  are changed to their dimensionless equivalent,



$D_k^*$ , by dividing by the square of the particle size and by the shear strain rate.

Values of dimensionless diffusive coefficients indicated by kinetic gas theory and those determined in our experiments agree to within an order of magnitude (Table 3), which is perhaps surprising in light of the uncertainty in estimating  $u$  and the granular temperature. The ranges of  $D_k^*$  reported result from the ranges of  $e$  and  $v$  considered. Agreement is best in the bead experiments, as might be expected since the theory is strictly appropriate for only equigranular materials.

**Implications for field studies**

The agreement of mixing coefficients determined in our experiments with both those of other experiments and those predicted by kinetic theory provides motivation for applying these coefficients to basal tills of the geologic record, with the goal of estimating bed shear strain. More specifically, if it is assumed a priori that mixing at contacts between till units is the result of bed deformation, then the appropriate solution to the diffusion equation (Equation (1)) can be used to estimate  $\gamma$  from measured mixing profiles by using laboratory values of  $D$ . Here we present an example of the method applied to the contact between the Des Moines Lobe and Superior Lobe tills in east-central Minnesota.

A mixing profile (Fig. 10) was measured across the contact between these tills at a gravel pit approximately 20 km north of St Paul, Minnesota. At this location, till of the Superior Lobe is overlain by a thickness of approximately 2–3 m of basal till deposited by the Grantsburg Sublobe of the Des Moines Lobe. Samples were collected at 1–2 mm increments over a 2 m thick section centered at the visual contact between the two tills. The vertical location of each sample was measured with a point gauge anchored at the top of the section. Each sample was then wet-sieved in the laboratory to isolate the 0.4–1.0 mm size fraction. This fraction was split multiple times to obtain approximately 300–500 grains. Grains of shale, the selected index lithology, were then identified. These grains, as well as the total number of grains, were counted to establish a mixing profile.

The profile shows that mixing occurred between the two tills over a thickness of 40 mm, and that it was symmetric about the visual contact between the tills (Fig. 10). A good simplification, owing to the small thickness over which mixing occurred, is that the contact was positioned in till thick

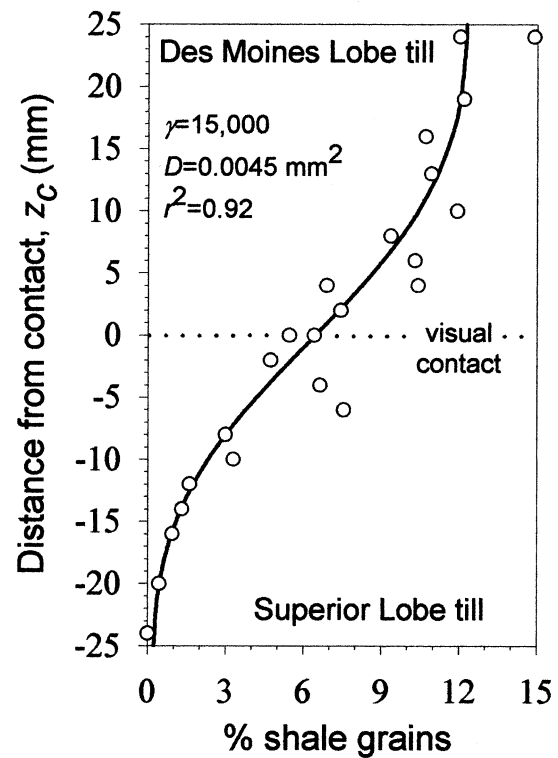


Fig. 10. Mixing profile measured across the contact of the Des Moines Lobe and Superior Lobe tills at a site 20 km north of St Paul, Minnesota. The maximum shear strain is determined by optimizing the fit of Equation (8) to the data using  $D = 0.0045 \text{ mm}^2$ , the minimum value determined in the ring-shear experiments.

enough relative to the zone of mixing to be considered infinite. The solution to Equation (1) then reduces to

$$C(z, \gamma) = C_1 C_2 + \frac{C_1}{2} \operatorname{erfc}\left(\frac{z_c}{2\sqrt{D\gamma}}\right) \quad (8)$$

(Crank, 1975, p. 12), where  $z_c$  is defined as the distance from the contact. Using  $D = 0.0045 \text{ mm}^2$ , the minimum value determined in our laboratory experiments, the best fit of Equation (8) to the field data using the method of least squares results in  $\gamma = 15\,000$ .

This estimate of  $\gamma$  is a maximum value, not only because a minimum value of  $D$  was used, but also because an initially smooth contact between the two till units is assumed in the calculation. An initially irregular contact would

Table 3. Parameters used in calculation of  $D_k^*$

Experiment No.	$u$	$c$	$\sigma$	$e$	$v$	$\dot{\gamma}$	$\gamma$	$D_k^*$ (from theory)	Mean $D^*$ (from experiments)
	$\text{mm s}^{-1}$	$\text{mm s}^{-1}$	mm			$\text{s}^{-1}$			
Bead 1	0.014	0.0071	0.8	0.85–1.0	0.6–0.7	$6.41 \times 10^{-4}$	57	0.052–0.145	0.128
Bead 2	0.013	0.0064	0.8	0.85–1.0	0.6–0.7	$4.93 \times 10^{-4}$	225	0.062–0.171	0.039
Bead 3	0.013	0.0063	0.8	0.85–1.0	0.6–0.7	$3.95 \times 10^{-4}$	142	0.076–0.211	0.078
Bead 4	0.015	0.0073	0.8	0.85–1.0	0.6–0.7	$3.76 \times 10^{-4}$	270	0.093–0.257	0.219
Till 1	0.013	0.0063	0.7	0.85–1.0	0.6–0.7	$3.58 \times 10^{-4}$	39	0.095–0.263	0.378
Till 2	0.027	0.0134	0.7	0.85–1.0	0.6–0.7	$6.51 \times 10^{-4}$	406	0.111–0.309	0.026
Till 3	0.013	0.0063	0.7	0.85–1.0	0.6–0.7	$3.14 \times 10^{-4}$	189	0.108–0.301	0.068
Till 4	0.013	0.0065	0.7	0.85–1.0	0.6–0.7	$4.35 \times 10^{-4}$	151	0.081–0.226	0.284
Till 5	0.014	0.0071	0.7	0.85–1.0	0.6–0.7	$5.10 \times 10^{-4}$	1032	0.076–0.211	0.014

result in more apparent mixing at lower strains and thus would reduce the calculated value of  $\gamma$ . The contact between these tills is, indeed, locally irregular (Chernicoff, 1983), although it is impossible to know its original geometry. We thus make no attempt to place a lower limit on shear strain across the contact. This is also warranted because we cannot rule out the possibility that mixing occurred by some other mechanism, such as by the plowing of clasts that may accompany accretion of lodgment till.

An important assumption of this method is that deformation was uniform across the contact. It is possible, however, that the underlying Superior Lobe till was overconsolidated when the Des Moines Lobe advanced over it and, hence, that it was stronger than the overlying till deposited by the Des Moines Lobe. This might have tended to focus strain in the upper till and to thereby impede mixing, resulting in an underestimate of  $\gamma$  near the contact. If this had been the case, however, asymmetry would be expected in the mixing profile. No such asymmetry is apparent in Figure 10, and thus there is no evidence from the mixing profile that deformation across the contact was non-uniform. This is not surprising. All that would be required to initiate deformation of the lower till would be a period of sufficiently low effective pressure caused by high pore-water pressure. Since water pressure may vary through orders of magnitude beneath glaciers, and sediment strengthening from overconsolidation is at most about 35% (compare ultimate and peak friction angles in Lambe and Whitman, 1969, p. 149), under some conditions both the upper and lower tills likely deformed. Dilation of the lower till during such periods would, after fairly small strains (Lambe and Whitman, 1969, p. 131), increase its porosity to a steady (critical-state) value comparable to that of the overlying till. Therefore, if the Superior Lobe till was overconsolidated and hence unusually strong when overridden by the Des Moines Lobe, it probably did not remain overconsolidated very long.

Several other potential sources of uncertainty are likely minor. The first of these is whether small-scale, experimental  $D$  values can be applied to larger-scale shear zones in the field. The principal concern is whether the removal of large clasts from till in the experiments affects mixing. Since these clasts constitute <2% of the till by volume, this is unlikely. Comminution of the index lithology with shear strain may also introduce uncertainty. Comminution, however, should have influenced mixing profiles only if deformation, and hence comminution, were not uniform with depth. Then, for example, more of the 0.4–1.0 mm size fraction might be lost at one depth than would be lost at another. As noted earlier, however, the mixing profiles provide no evidence of non-uniform deformation, as indicated by the good fit of the diffusion model to the field data. A final uncertainty arises from the potential influences of effective stress and shear strain rate on mixing, which may vary widely subglacially. As noted earlier, the similarity of our  $D^*$  values to those of other studies conducted at much different stresses and rates (Scott and Bridgwater, 1976; Stephens and Bridgwater, 1978) indicates that variations in these parameters are relatively unimportant.

Finally, a limitation of the method is that it can be used to estimate shear strain only near contacts between till units. Strain that may have occurred above or below contacts will obviously not contribute to mixing between tills. All indicators of strain in sediment and rocks are, of course, subject to this same limitation: strain can be estimated only where there are markers for doing so.

## CONCLUSIONS

Diffusive mixing occurs between two layers of granular material undergoing simple shear parallel to their contact, and ring-shear experiments provide the value of the only fitted parameter in the linear theory that describes such mixing: the mixing coefficient,  $D$ . The value of  $D$  decreased with strain in experiments with till, due either to an irregular initial contact or to the focusing of deformation away from the contact at high strains. Dimensionless values of  $D$  determined in these experiments are comparable to those determined in other experiments conducted at different strain rates and effective stresses (e.g. Stephens and Bridgwater, 1978), and kinetic theory provides an estimate of the dimensionless mixing coefficient that is within an order of magnitude of laboratory values.

The laboratory determination of  $D$  allows an upper limit to be placed on bed shear strain from the distribution of index lithologies measured across till contacts in the field. A preliminary application of this technique at one field site, where the contact between the Des Moines Lobe and Superior Lobe till is exposed, indicates a maximum shear strain of 15 000 at the depth of the contact. Such information cannot be inferred from conventional strain indicators in till, which either stop changing at low strains (e.g. clast fabric) or are obliterated if strain becomes too large.

## ACKNOWLEDGEMENTS

We thank D. Nelsen, D. Salisbury and N. Davis for bead and particle counting. We also thank R. B. Alley for helpful criticism. This work was supported by U.S. National Science Foundation grant OPP-9530814.

## REFERENCES

- Alley, R. B. 1991. Deforming-bed origin for southern Laurentide till sheets? *J. Glaciol.*, **37**(125), 67–76.
- Boulton, G. S. 1996. Theory of glacial erosion, transport and deposition as a consequence of subglacial sediment deformation. *J. Glaciol.*, **42**(140), 43–62.
- Bridgwater, J. 1980. Self-diffusion coefficients in deforming powders. *Powder Technol.*, **25**(1), 129–131.
- Bridgwater, J., W. S. Foo and K. J. Stephens. 1985. Particle mixing and segregation in failure zones-theory and experiment. *Powder Technol.*, **41**(2), 147–158.
- Carnahan, N. F. and K. E. Starling. 1969. Equations of state for non-attracting rigid spheres. *J. Chem. Phys.*, **51**, 635–636.
- Chernicoff, S. E. 1983. Glacial characteristics of a Pleistocene ice lobe in east-central Minnesota. *Geol. Soc. Am. Bull.*, **94**(12), 1401–1414.
- Clark, P. U. 1994. Unstable behavior of the Laurentide ice sheet over deforming sediment and its implications for climate change. *Quat. Res.*, **41**(1), 19–25.
- Clark, P. U. 1997. Sediment deformation beneath the Laurentide ice sheet. In Martini, I. P., ed. *Late glacial and postglacial environmental changes: Quaternary, Carboniferous-Permian and Proterozoic*. New York, Oxford University Press, 81–97.
- Clark, P. U. and J. S. Walder. 1994. Subglacial drainage, eskers, and deforming beds beneath the Laurentide and Eurasian ice sheets. *Geol. Soc. Am. Bull.*, **106**(2), 304–314.
- Clark, P. U., J. M. Licciardi, D. R. MacAyeal and J. W. Jenson. 1996. Numerical reconstruction of a soft-bedded Laurentide ice sheet during the last glacial maximum. *Geology*, **24**(8), 679–682.
- Clayton, L., D. M. Mickelson and J. W. Attig. 1989. Evidence against pervasively deformed bed material beneath rapidly moving lobes of the southern Laurentide ice sheet. *Sediment. Geol.*, **62**(3–4), 203–208.
- Crank, J. 1975. *The mathematics of diffusion*. Second edition. Oxford, Clarendon Press.
- Dowdeswell, J. A. and M. J. Siegert. 1999. Ice-sheet numerical modelling and marine geophysical measurements of glacier-derived sedimentation on the Eurasian Arctic continental margins. *Geol. Soc. Am. Bull.*, **111**(2), 1080–1097.
- Hart, J. K. 1994. Till fabric associated with deformable beds. *Earth Surf.*

- Processes Landforms*, **19**(1), 15–32.
- Hart, J. K. 1995. Subglacial erosion, deposition and deformation associated with deformable beds. *Prog. Phys. Geogr.*, **19**(2), 173–191.
- Hart, J. K. 1997. The relationship between drumlins and other forms of subglacial glaciotectionic deformation. *Quat. Sci. Rev.*, **16**(1), 93–107.
- Hart, J. K. and G. S. Boulton. 1991. The interrelation of glaciotectionic and glaciodepositional processes within the glacial environment. *Quat. Sci. Rev.*, **10**(4), 335–350.
- Hart, J. K. and D. H. Roberts. 1994. Criteria to distinguish between subglacial glaciotectionic and glaciomarine sedimentation: I. Deformation styles and sedimentology. *Sediment. Geol.*, **91**(1–4), 191–213.
- Head, K. H. 1989. *Soil technician's handbook*. New York, etc., John Wiley and Sons.
- Hicock, S. R. and A. Dreimanis. 1992. Deformation till in the Great Lakes region: implications for rapid flow along the south-central margin of the Laurentide ice sheet. *Can. J. Earth Sci.*, **29**(7), 1565–1579.
- Hiemstra, J. F. and J. J. M. van der Meer. 1997. Pore-water controlled grain fracturing as an indicator for subglacial shearing in tills. *J. Glaciol.*, **43**(145), 446–454.
- Hooke, R. LeB. and A. Elverhoi. 1996. Sediment flux from a fjord during glacial periods, Isfjorden, Spitsbergen. *Global and Planetary Change*, **12**(1–4), 237–249.
- Hooyer, T. S. 1999. Laboratory studies of till deformation with implications for the flow mechanism of the Des Moines Lobe. (Ph.D. thesis, Iowa State University)
- Hooyer, T. S. and N. R. Iverson. 2000. Clast-fabric development in a shearing granular material: implications for subglacial till and fault gouge. *Geol. Soc. Am. Bull.*, **112**(5), 683–692.
- Hsiau, S. S. and M. L. Hunt. 1993. Kinetic theory analysis of flow-induced particle diffusion and thermal conduction in granular material flows. *J. Heat Transfer*, **115**(3), 541–548.
- Iverson, R. H. 1997. The physics of debris flows. *Rev. Geophys.*, **35**(3), 245–296.
- Iverson, N. R., T. S. Hooyer and R. LeB. Hooke. 1996. A laboratory study of sediment deformation: stress heterogeneity and grain-size evolution. *Ann. Glaciol.*, **22**, 167–175.
- Iverson, N. R., R. W. Baker and T. S. Hooyer. 1997. A ring-shear device for the study of till deformation: tests on tills with contrasting clay contents. *Quat. Sci. Rev.*, **16**(9), 1057–1066.
- Iverson, N. R., T. S. Hooyer and R. W. Baker. 1998. Ring-shear studies of till deformation: Coulomb-plastic behavior and distributed strain in glacier beds. *J. Glaciol.*, **44**(148), 634–642.
- Jenkins, J. T. and S. B. Savage. 1983. A theory for the rapid flow of identical, smooth, nearly elastic spherical particles. *J. Fluid Mech.*, **130**, 187–202.
- Jenson, J., P. U. Clark, D. R. MacAyeal, C. Ho and J. C. Vela. 1995. Numerical modelling of advective transport of saturated deforming sediment beneath the Lake Michigan lobe, Laurentide ice sheet. *Geomorphology*, **14**(2), 157–166.
- Jenson, J. W., D. R. MacAyeal, P. U. Clark, C. L. Ho and J. C. Vela. 1996. Numerical modeling of subglacial sediment deformation: implications for the behavior of the Lake Michigan lobe, Laurentide ice sheet. *J. Geophys. Res.*, **101**(B4), 8717–8728.
- Kemmis, T. J. 1981. Importance of the regelation process to certain properties of basal tills deposited by the Laurentide ice sheet in Iowa and Illinois, U.S.A. *Ann. Glaciol.*, **2**, 147–152.
- Lambe, T. W. and R. V. Whitman. 1969. *Soil mechanics*. New York, etc., John Wiley and Sons.
- Lun, C. K. K. and S. B. Savage. 1986. The effects of impact velocity dependent coefficient of restitution on stresses developed by sheared granular materials. *Acta Mech.*, **63**(1–4), 15–44.
- Lun, C. K. K., S. B. Savage, D. J. Jeffrey and N. Chepuruiy. 1984. Kinetic theories for granular flow: inelastic particles in Couette flow and slightly inelastic particles in a general flowfield. *J. Fluid Mech.*, **140**, 223–256.
- Mandl, G., L. N. J. de Jong and A. Maltha. 1977. Shear zones in granular material — an experimental study of their structure and mechanical genesis. *Rock Mech.*, **9**, 95–144.
- Menzies, J. and A. J. Maltman. 1992. Microstructures in diamictites: evidence of subglacial bed conditions. *Geomorphology*, **6**(1), 27–40.
- Menzies, J., K. Zaniewski and D. Dreger. 1997. Evidence, from microstructures, of deformable bed conditions within drumlins, Chimney Bluffs, New York State. *Sediment. Geol.*, **111**(1–4), 161–176.
- Piotrowski, J. A. and A. M. Kraus. 1997. Response of sediment to ice-sheet loading in northwestern Germany: effective stresses and glacier-bed stability. *J. Glaciol.*, **43**(145), 495–502.
- Savage, S. B. 1987. Interparticle percolation and segregation in granular material: a review. In Selvadurai, A. P. S., ed. *Developments in engineering mechanics*. Amsterdam, etc., Elsevier, 347–363.
- Savage, S. B. 1993. Disorder, diffusion and structure formation in granular flows. In Bideau, D., ed. *Disorder and granular media*. Amsterdam, etc., Elsevier Science Publishers, 255–285.
- Savage, S. B. and D. J. Jeffrey. 1981. The stress tensor in a granular flow at high shear rates. *J. Fluid Mech.*, **110**, 255–272.
- Scott, A. M. and J. Bridgwater. 1976. Self-diffusion of spherical particles in a simple shear apparatus. *Powder Technol.*, **14**(1), 177–183.
- Shackelford, C. D. 1991. Laboratory diffusion testing for waste disposal: a review. *Journal of Contaminant Hydrology*, **7**(3), 177–217.
- Steel, R. G. D., J. H. Torrie and D. A. Dickey. 1997. *Principles and procedures of statistics: a biometrical approach*. New York, McGraw-Hill.
- Stephens, D. J. and J. Bridgwater. 1978. The mixing and segregation of cohesionless particulate materials. Part II. Microscopic mechanisms for particles differing in size. *Powder Technol.*, **21**(1), 29–44.
- Van der Meer, J. J. M. 1993. Microscopic evidence of subglacial deformation. *Quat. Sci. Rev.*, **12**(7), 553–587.
- Van der Meer, J. J. M. 1997. Particle and aggregate mobility in till: microscopic evidence of subglacial processes. *Quat. Sci. Rev.*, **16**(8), 827–831.

*MS received 18 January 2000 and accepted in revised form 14 August 2000*